Addressing Reproducibility Challenges in High-Throughput Photochemistry

Brenda Pijper,[†] Lucía M. Saavedra,[†] Matteo Lanzi,[‡] Maialen Alonso,[†] Alberto Fontana,[†] Marta Serrano,[†] José Enrique Gómez,[†] Arjan W. Kleij,[‡, §] Jesús Alcázar,[†] Santiago Cañellas [†,*]

[†] Chemical Capabilities, Analytical & Purification, Global Discovery Chemistry. Janssen-Cilag, S.A., E-45007 Toledo, Spain

[‡] Institute of Chemical Research of Catalonia (ICIQ), the Barcelona Institute of Science and Technology, Av. Països Catalans 16, 43007 Tarragona, Spain

[§] Catalan Institute of Research and Advanced Studies (ICREA), Pg. Lluís Companys 23, 08010 Barcelona, Spain

Supporting Information Placeholder

Light-mediated reactions have emerged as an indispensable tool in organic synthesis and drug discovery, enabling novel transformations and providing access to previously unexplored chemical space. Despite their widespread application in both academic and industrial research, the utilization of light as an energy source still encounters challenges regarding reproducibility and data robustness. Herein we present a comprehensive head-to-head comparison of commercially available batch photoreactors, alongside the introduction of the use of batch and flow photoreactors in parallel synthesis. Hence, we aim to establish a reliable and consistent platform for light-mediated reactions in high-throughput mode. Herein, we showcase the identification of several platforms aligning with the rigorous demands for efficient and robust high-throughput experimentation screenings and library synthesis.

Inspired by natural photochemical processes,[1] the recent emergence of photoredox catalysis has revolutionized synthetic organic chemistry. This breakthrough enables controlled and selective access to high-energy intermediates, facilitating previously unattainable bond formations and novel chemical pathways.[2–6] Consequently, light-mediated transformations have profoundly impacted various research fields, with many incorporating this energy source into their standard toolbox. As an example, medicinal chemists have embraced photochemistry within drug discovery programs transforming synthetic disconnections by introducing innovative processes such as C(sp^3)-C(sp^2), C(sp^3)-C(sp^3), C-N, or C-O bond-forming methods, among others.[7–10]

The increasing complexity of active pharmaceutical ingredients (API) and the pressing need to expedite medicinal chemistry programs to clinical stages have spurred the establishment and development of high-throughput approaches. These approaches aim to identify optimal reaction conditions for elaborated scaffolds, advance automated parallel medicinal chemistry (PMC) for library synthesis, and generate high-quality data sets under consistent reaction conditions for the development synthesis predictive models.[11]

Despite the demonstrated value of light mediated processes in organic chemistry and drug discovery, reproducibility and reliability remain challenging. Spectral output, light intensity, light path length, and temperature vary across reactors and significantly impact data consistency and yields. Similar challenges have been encountered and successfully addressed in the field of microwave irradiation.[12] Achieving uniformity and reproducibility is a challenge with single-position photoreactors, and it becomes more complex for high-throughput photoreactors.[13–17]

To establish a baseline and tackle the challenges associated with high-throughput photochemical reactions and light-mediated parallel synthesis, we compared commercially available batch and flow photoreactors across a uniform series of assessments. We then explored the use photo-parallel synthesis in batch and flow setups for a real-case scenario and library synthesis of drug-like molecules using a recently developed C(sp^3)-C(sp^2) bond-forming methodology. [18] Taken together, these results provide a practical guide for where and when the different photoreactors are most effective.

Batch setups

In batch reactors, factors such as the distance from the light source, vessel geometry, and the path length directly influence the light penetration, per the Lambert-Beer law. Achieving homogeneous exposure of reactants to photons requires effective mixing, often achieved by mechanical stirring or orbital shaking. Additionally, precise control of the reaction temperature is fundamental for both desired and undesired reaction pathways. While distance to the light source and geometry are determined by photoreactor design, the path length can be adjusted by varying reaction volume based on the vessel geometry. In this comparative study, all reactions used the same path length to ensure data consistency (See SI Table S1). Reactors were utilized as supplied from vendors without structural modifications and were equipped with air-cooling or liquid-cooling systems when feasible. Eight photoreactors' performance was evaluated based on starting material, desired product, byproducts, reaction temperature, and well-to-well consistency (Table 1).

***Table 1**: Commercially available photoreactors setups and their features; λ max: irradiation wavelength. Ww: light power per well. Nw: number of wells. Data provided by the vendors.*

	Commercial name[a]	λ max (nm)	Ww (mW)	Nw
P1	Penn PhD Photoreactor M2	450	3400	5
P2	Lumidox 24 GII	445	885	24
P3	Luzchem WPI	462	51.5	24
P4	SynLED Parallel	465-470	135	24
P5	HepatoChem EvoluChem PhotoRedOx Box	450	3750	8
P6	Lumidox 48 Well Temperature Controlled Reactor (TCR)	470	345	48
P7	TT-HTE 48 Photoreactor	447	2328	48
P8	Lumidox II 96-Well LED Arrays	445	415	96

We initiated our investigation by selecting the Amino Radical Transfer (ART) coupling as our model reaction (Figure 1a). This choice was deliberate and based on several considerations. The ART coupling holds significant relevance to the pharmaceutical industry, as its ability to increase F(sp^3) of drug candidates onto (hetero)aromatic scaffolds.[19] Moreover, the ART coupling is not sensitive to moisture or oxygen, thereby avoiding additional interfering factors that could complicate the analysis of events related to light irradiation. Importantly, to evaluate the influence of various configurations on the reaction kinetics, the reactions were conducted for a short period of time resulting in partial conversion of the starting materials.[20]

All the tested photoreactors demonstrated the ability to facilitate the desired ART coupling within 5 minutes of reaction time (Figure 1c). Variability in conversion was observed both across the positions of individual reactors, and across the different photoreactor designs, emphasizing the significant impact of design on the reaction outcome and the importance of meticulously reporting procedures and setups. Based on the measured conversions, photoreactors were classified into three categories.

The first category comprises of photoreactors **P1**, **P3**, **P4,** and **P5**, which consistently exhibited low conversion rates (<35%), accompanied by varying levels of selectivity over byproducts (Figure 1f). These photoreactors also demonstrated differences in temperature control, with temperatures ranging from 26 to 46 ºC only after 5 minutes of reaction time. Additionally, irradiation homogeneity varied withing this category, with standard deviations ranging from 0.3 to 3.2% of product **3**).

The second category comprises setups **P2** and **P8**, which yielded the highest reaction yields (approx. 65% after 5 min in both cases) with uniform outcomes across the plates (standard deviation: 0.9-1.2% of product **3**). However, achieving high conversion of **1** (>90%) came at the expense of a significant amount of side product formation (31% and 38% respectively). This reduced selectivity may be attributed to inadequate temperature control leading to undesired thermal pathways, despite efforts to provide an external cooling jacket (temperatures ranging from 46-47 ºC after 5 min; additional temperature measurements at 30 min revealed internal temperatures continued to rise, reaching 60-65 ºC).

The third class of photoreactors includes **P6** and **P7**, which notably enhanced reaction control, resulting in approximately 40% product (**3**) formation and 50% conversion of starting material **1**, with consistent yield homogeneity across the 48 wells (standard deviation: 1.8-2.3%). Importantly, these two photoreactors feature a built-in liquid cooling circulation, enabling precise control of the internal temperature (15 and 16 ºC, respectively, after 5 minutes, remaining stable after 30 min). This meticulous temperature control reflects in a lower level of side-products formation through thermal pathways, approximately 10%.

Further exploration into photoreactors for HTE campaigns, led us to focus on photoreactors **P6** and **P7** due to their excellent temperature control and robustness across the plate after a 5 min reaction time. In subsequent investigations, the ART coupling reaction was repeated to achieve full conversion of **1** which was achieved in 30 min of irradiation for both systems, resulting in approximately 70% product formation across the plates (Figure 1g). Consistency in reaction outcomes was also observed for **P6** and **P7**, with a maximum standard deviation of 2.3 % and 1.2 %, respectively. Complementary C(sp^2)-C(sp^3) bond-forming couplings, such as photocatalyzed cross-electrophile coupling (XEC) and a decarboxylative coupling, were also explored with photoreactors **P6** and **P7**.[21–24] Comparable average yields across the plates were obtained for both XEC and the decarboxylative coupling reactions (See SI Table S12 and S15). In conclusion, photoreactors **P6** and **P7** show promise as platforms for light mediated HTE screenings, facilitating 48 parallel reactions while maintaining accuracy in the recorded data and precise temperature control. However, integrating current plate layouts with automated workflows presents challenges. Adhering to a standard SBS format would enhance compatibility with automated workflows and minimize the need for human intervention.

In addition to identifying a robust light source, automation has become crucial in reducing the inherent variability associated with human intervention, thereby enhancing reproducibility, productivity, and the quality of data acquisition. Furthermore, automation in parallel synthesis workflows is recognized for its ability to boost productivity and efficiency, accelerating the discovery cycles in medicinal chemistry. [13] With these considerations in mind, we embarked on developing an end-to-end automated and user-friendly high-throughput workflow, named PhotoPlay&GO. This innovative approach integrates a liquid handler and a photoreactor, requiring minimal human intervention. To our knowledge, automated platforms for light-mediated parallel synthesis remains unexplored.

Capitalizing on the success of the previously validated ART coupling, we opted to construct our PhotoPlay&GO workflow around a Tecan liquid handler (Freedom EVO200, air LiHa equipped with disposable tips) integrated with an alligator magnetic vertical tumble stirrer featuring a recirculating fluid block (capable of operating up to -70°C) connected to an external chiller, alongside a commercially available parallel photoreactor (Figure 2a).

***Figure 1**: (a) Scheme of the ART coupling with aryl bromide **1** and aliphatic boronic ester **2** using eight commercial parallel photoreactors; (b). Commercial names; (c). Heat map of the product formation in each photoreactor; (d) Pictures of the photoreactors; (e) Product distribution featuring starting material (SM), desired product **3** (P) and the sum of byproducts (Other, e.g. protodehalogenation or C-N coupling of morpholine among other unidentified peaks); (f) Parameters measured after 5 minutes irradiation, including the internal reaction temperature, average yield and standard deviation (see SI for more details); (g) Comparison of the product yields after 30 minutes between the Lumidox TCR (**P6**) and the TT-HTE 48 (**P7**) setups.*

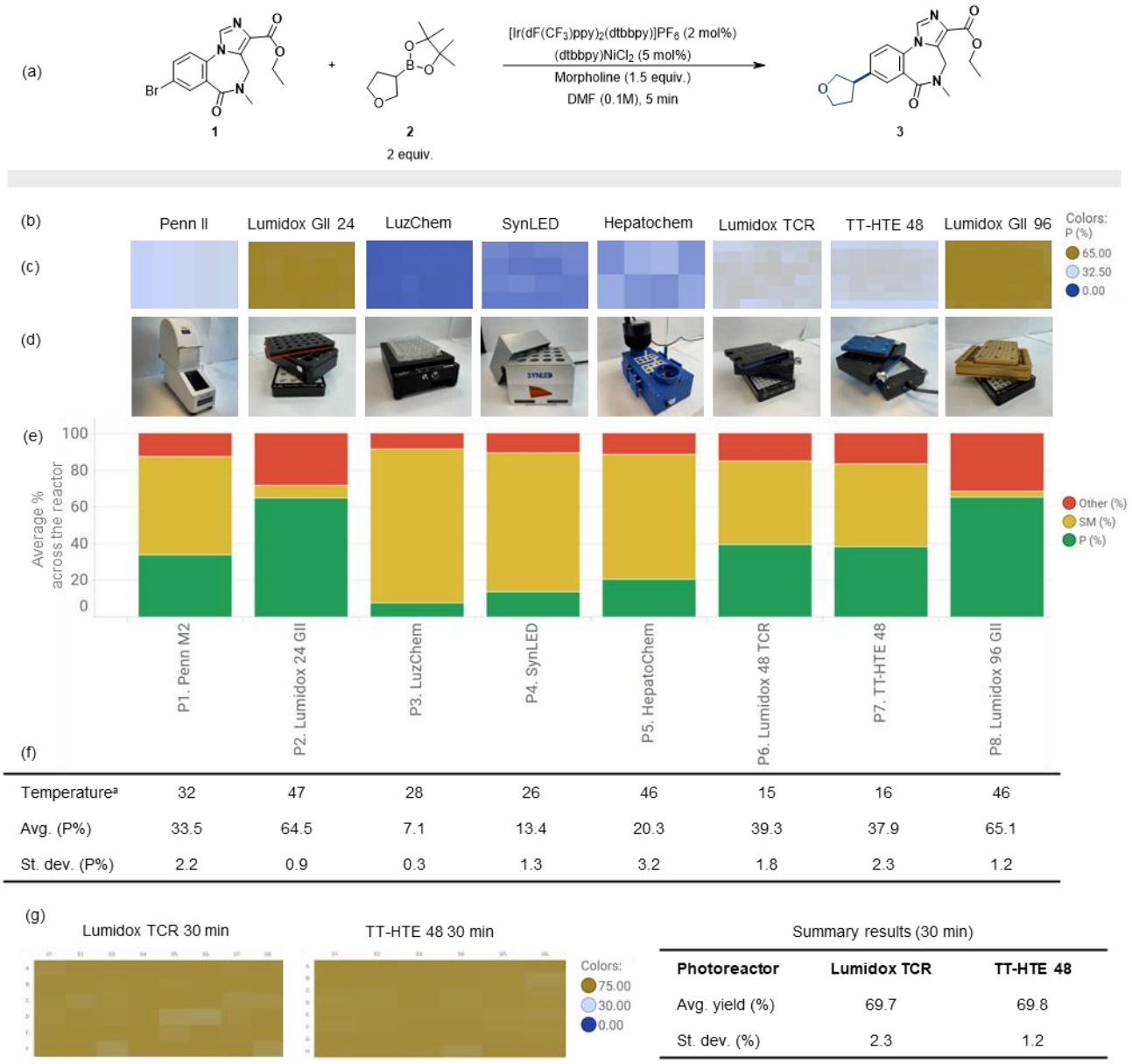

	P1. Penn M2	P2. Lumidox 24 GII	P3. LuzChem	P4. SynLED	P5. HepatoChem	P6. Lumidox 48 TCR	P7. TT-HTE 48	P8. Lumidox 96 GII
Temperature[a]	32	47	28	26	46	15	16	46
Avg. (P%)	33.5	64.5	7.1	13.4	20.3	39.3	37.9	65.1
St. dev. (P%)	2.2	0.9	0.3	1.3	3.2	1.8	2.3	1.2

Summary results (30 min)

Photoreactor	Lumidox TCR	TT-HTE 48
Avg. yield (%)	69.7	69.8
St. dev. (%)	2.3	1.2

Considering the typical large scale demanded for parallel synthesis, we selected **P2** for its homogeneous irradiation and high yields achievable within just 5 minutes. Operationally, the reactions were conducted on a 200 µmol scale in 1-dram vials containing the pre-weighed radical precursors (2.0 equivalents of the respective alkyl-Bpin) arranged in a 24-well plate (SBS format). The workflow commenced with the automated addition of a pre-prepared 0.1 M DMF stock solution of the nickel precursor, iridium photocatalyst, aryl halide, and morpholine across the entire plate. Stirring and irradiation by blue LEDs (445 nm) were then applied for 30 minutes to ensure complete conversion of all the utilized building blocks. Heat dissipation was facilitated by a recirculating fluid block connected to an external chiller, maintaining the internal temperatures at 60 ºC, even though the set temperature was 10 ºC.

We commenced our study by utilizing 24 alkyl pinacol boronic esters (Bpins) (**3** – **26**) along with an aryl bromide **1** derived from Flumazenyl. Encouragingly, 21 out of 24 building blocks yielded acceptable results for standard medicinal chemistry synthesis (>10% isolated yield after using automated high-throughput purification platforms) within a timeframe of less than 2 hours. Including reaction set-up, irradiation, work-up, and preparation of analysis and purification plates, all accomplished without any human intervention (Figure 2b).

***Figure 2**: (a) Instrumental composition of the PhotoPlay&Go: (1) disposable tips, (2) solvent/solution troughs, (3) scavenger, (4) vacuum manifold, (5) analysis plate, (6) reaction plate; (b) Parallel synthesis: alkyl boronic ester scope; (c) Parallel synthesis: (hetero)aryl halide scope. [a] LMCS conversion. [b] Isolated HTP yield.*

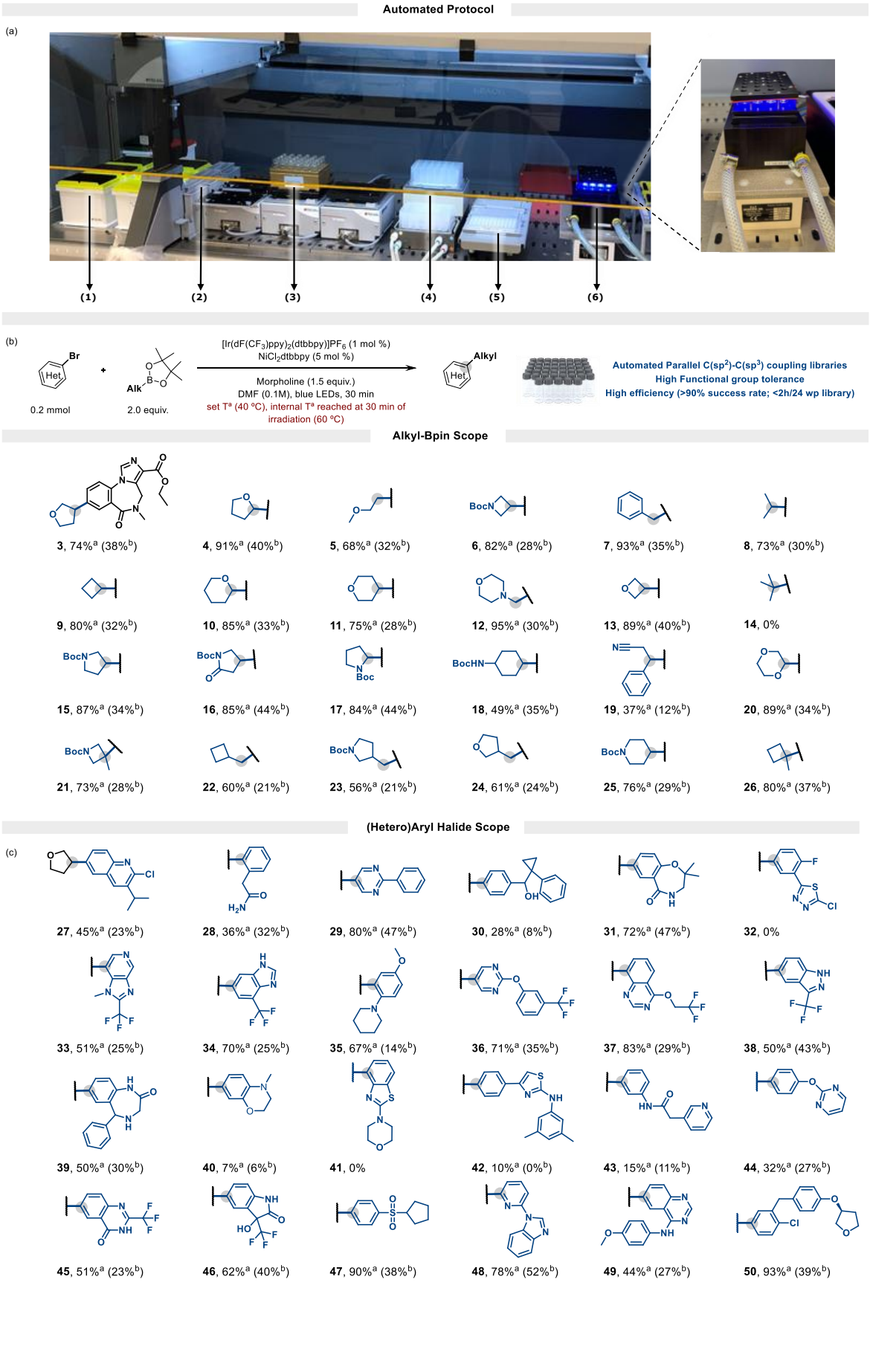

Remarkably, our protocol demonstrated tolerance towards primary, secondary, and even challenging tertiary alkyl substrates for nickel photoredox chemistry, with few exceptions like the *tert*-butyl group (**14**). Moreover, primary and secondary benzylic C(sp^3) centers were successfully introduced under these conditions using the model aryl bromide **1**. The throughput of our automated protocol prompted us to further explore the scope of aryl halides for potential medicinal chemistry applications (Figure 2c). To this end, we carefully selected 24 drug-like aryl halide scaffolds (**27** – **50**) encompassing a diverse range of heterocycles, hydrogen-bond donors/acceptors, varying degrees of polarity, and functional groups such as amides, carbonyls, protic, and trifluoro moieties. This allowed us to thoroughly probe the methodological coupling process across a more comprehensive chemical space. Upon subjecting these aryl halides to our PhotoPlay&GO protocol, we observed that 20 out of 24 aryl halides provided encouraging results, yielding greater than 10% isolated yield in a PMC setting. Notably, various heterocycles and functional groups, including primary and secondary amides, unprotected benzimidazoles, nitriles, pyridines, sulfones and even aryl chlorides, were well-tolerated under the reaction conditions.

Flow setups

After exploring various batch photochemistry tools, we opted to assess flow photochemistry as a complementary approach to the PhotoPlay&GO. Flow chemistry has emerged as a compelling solution to address reproducible issues in photochemistry because of small path-length tubing which enhances light penetration, in accordance with the Lambert-Beer law. Additionally, the substantial surface-to-volume ratio facilitates precise control over reaction temperature. Furthermore, flow chemistry enables meticulous management of reaction parameters such as wavelength, light intensity, pressure, and irradiation time. [25–27] Despite these advantages, most instances in the literature employ flow chemistry for large scale synthesis, where steady-state conditions are achieved, and dispersion is minimized.[28–32]

Figure 3*. Optimization conducted on the plate-to-plate approach providing a comprehensive overview of the optimization efforts undertaken to fine-tune the reaction conditions in flow (a) Screening of 24 ligand and 4 amine activators, (b) Follow-up screening of nickel sources and amine activator, (c) Screening of equivalents and (d) Screening of residence time, light intensity, and temperature, focusing on the two best nickel sources.*

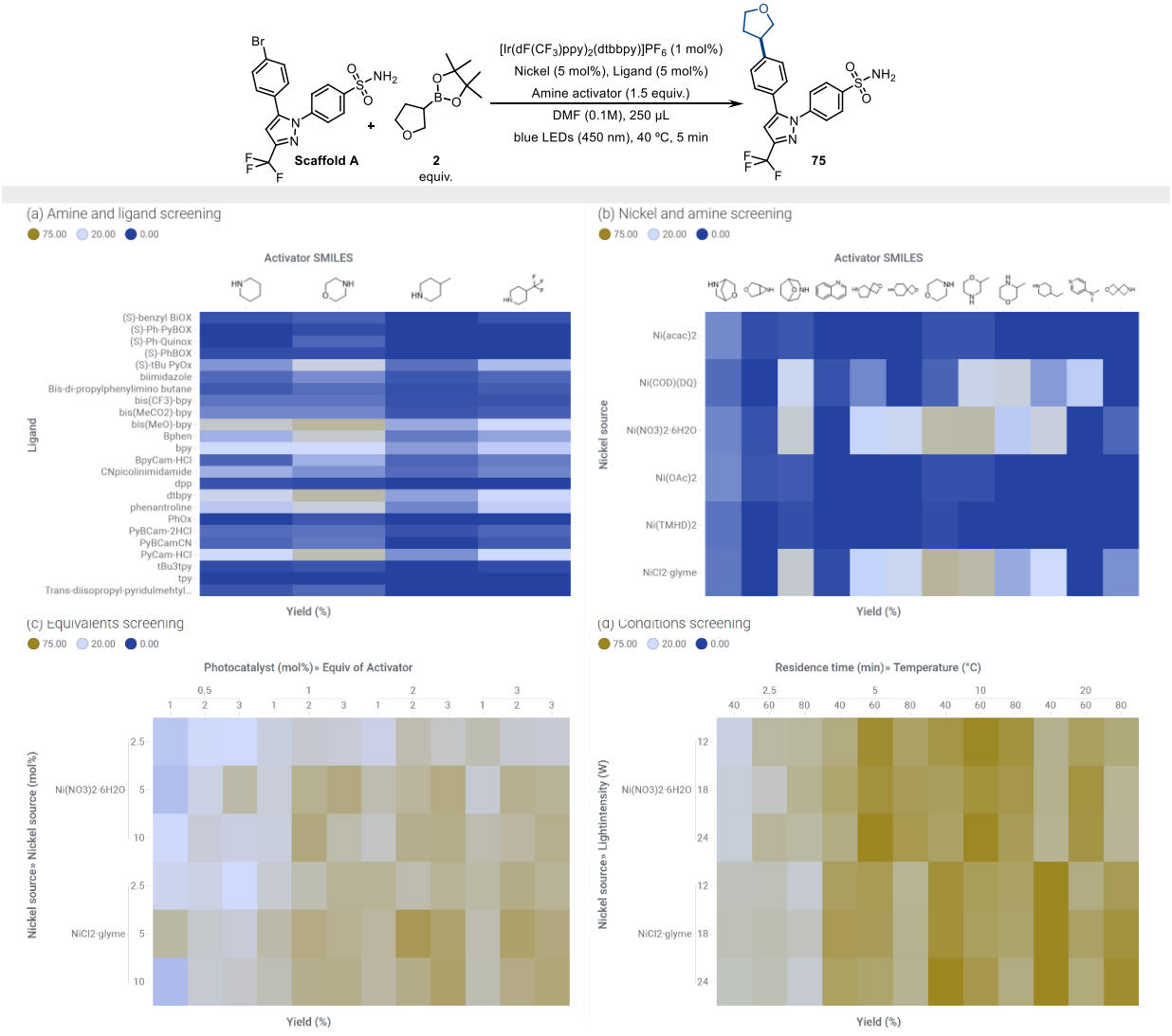

The application of flow photochemistry in High-Throughput Experimentation (HTE) and library synthesis has been constrained due to dispersion effects. Only a handful of platforms have been described employing slug flow approaches, and to date, a singular platform combining HTE and library synthesis in flow remains unreported.[33–39] Moreover, translating chemistry protocols from batch to flow presents challenges due to the differences in kinetics. To facilitate direct HTE in flow, which involves running sequential experiments, we embarked on optimizing the process. Our objective is minimizing the residence time while achieving high yields to maximize productivity as number of experiments per unit time.

Initially, we adapted the Automated Vapourtec R2/R4 system to the SBS format using a Gilson 205 rack holder, seamlessly integrating it into our J&J's modular automated (SBS) platform.[40] As a model substrate for the ART coupling, we selected scaffold (**A**) (figure 3), which is a Pfizer drug marketed as COX-2 inhibitor (Celebrex).[41] Following a preliminary residence time screening at 2, 5 and 10 minutes at 40 ºC, we achieved 49% assay yield within 5 minutes, enabling efficient high-throughput experimentation (SI Table S18).[42] Subsequently, we investigated the minimum injection volume feasible in the flow setup by performing 48 reactions with three distinct injection volumes (100, 250, and 500 µL at 0.1 M concentration, SI Figure S18). Results indicated that at a 100 µL injection volume, the dispersion effect hampered the reaction. Conversely, while 250 µL resulted in slightly lower conversion rates compared to 500 µL, it offers the advantage of conserving precious starting material, thus minimizing material usage.

Reproducibility and robustness were evaluated by sequentially running the same reaction using the UV-150 flow reactor from Vapourtec (450 nm, 24 W). Initial attempts (SI Figure S20) showed a standard deviation of 2.7% over 96 experiments, with a variation of 7.2%. However, a decrease in yield was observed over time, possibly due to degradation of components in the stock solution during the extended reaction time of 32 hours. To confirm this hypothesis, all possible reagent combinations were prepared and reacted immediately and after 72 hours of mixing (SI Figure S21). It was discovered that morpholine and the photocatalyst were incompatible, resulting in a significant loss of yield after 72 hours. Subsequently, testing two separated solutions- morpholine and aliphatic boronic ester in one line and the rest of the reagents in the other- over 96 experiments led to remarkably high reproducibility (variation of 2.5% and standard deviation of 1.6% in LCMS yield, SI figure S22).

With the robustness and the reproducibility of the flow setup confirmed, we proceeded to optimize the reaction by exploring various parameters in a 96-well plate format. These parameters included the metal source, catalyst ligand, amine activator, reaction stoichiometry, reaction temperature, reaction time and light intensity. We began the optimization through a combinatorial screening of 24-ligand and 4 different 6-membered amine activators bearing various substituents (Figure 3a).

Figure 4*. Substrate scope of the initial 24-member aliphatic pinacol boronic ester library in continuous flow.* [a] *LMCS conversion.* [b] *Isolated HTP yield.*

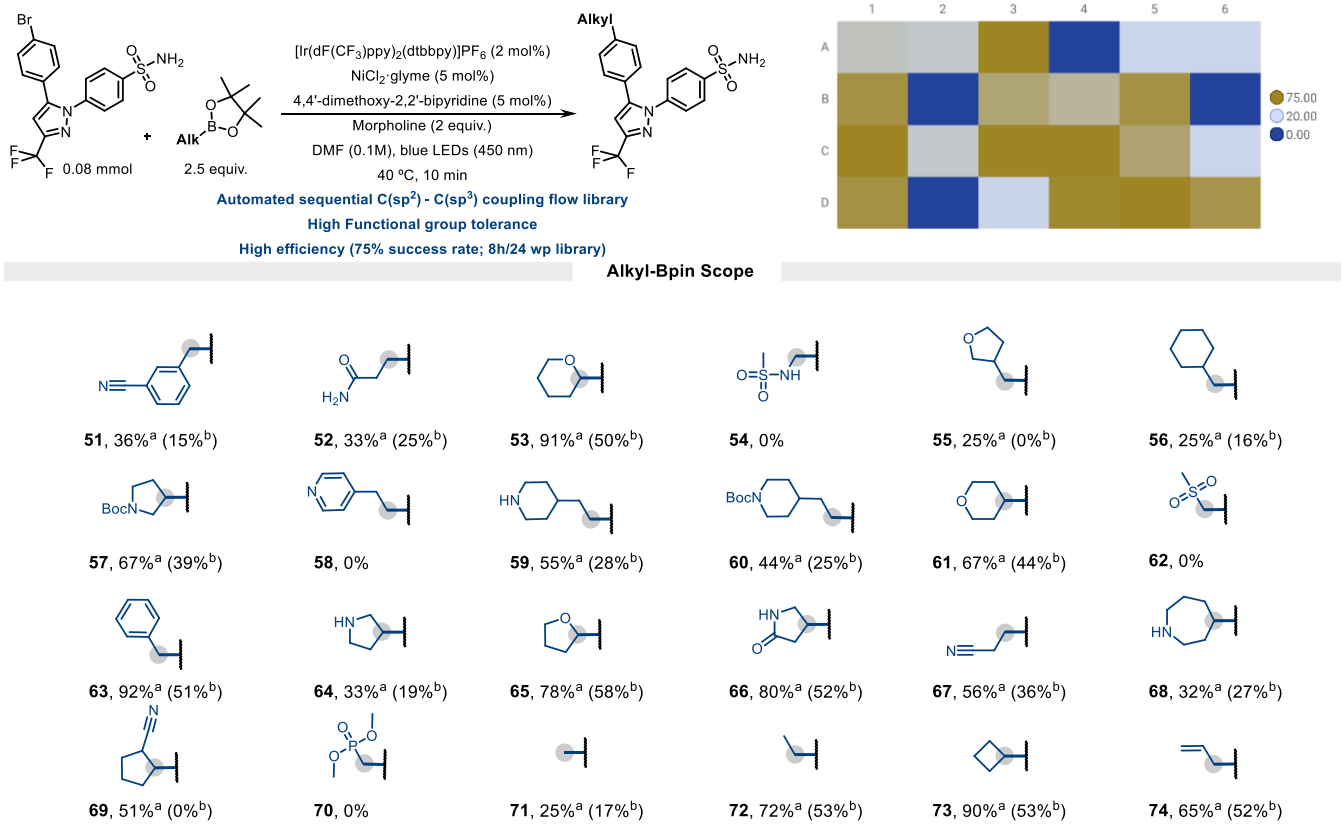

Superior yields were achieved with electron-rich bipyridine ligands, such as 4,4'-dimethoxybipyridine and dtbpy, in combination with morpholine, outperforming all tested piperidines (43% assay yield). Subsequently, we systematically examined 6 different nickel sources and 12 amine-based activators (Figure 3b). Morpholine in combination with $NiCl_2$·glyme and $Ni(NO_3)_2·6H_2O$ demonstrated similar yet superior results (43% assay yield) compared to all the other combination.[43,44] Harnessing the power of the HTE platform in flow, we screened the loadings of the photocatalyst (0.5, 1, 2, and 3 mol%) and morpholine (1, 2, and 3 equivalents) in combination with two nickel sources (2.5, 5, and 10 mol%) (Figure 3c). This analysis identified 5 mol% of $NiCl_2$·glyme, 2 equivalents of the morpholine and 2 mol% of the photocatalyst as optimal, with 75% yield. Fine-tuning of the residence time (2.5, 5, 10, and 20 minutes), light intensity (12, 18 and 24 W), and temperature (40, 60, and 80 ºC) established the optimal conditions as a 10-minute residence time, 40 ºC, and 24 W light intensity, yielding the desired product with a 77% yield (Figure 3d). Although a longer residence time (20 min at 40 °C) yielded better results (82%), a shorter reaction time is highly desirable in library synthesis, as it reduces the total run time. This plate-to-plate approach demonstrates the feasibility of conducting HTE experiments in flow, showcasing the flexibility of the set-up through combinatory screening of temperature, residence time, and light intensity for each run.

With the optimized conditions established, we proceeded to assess this platform for library synthesis at a preparative scale. Initially, we designed a 24-member library synthesis using the Scaffold (**A**) (Celebrex) in combination with a wide range of aliphatic boronic esters (Figure 4).

Figure 5. *96-member combinatorial library linking 12 aliphatic boronic esters and 8 drug-like (hetero)aryl scaffolds.* [a] *LMCS conversion.* [b] *Isolated HTP yield.*

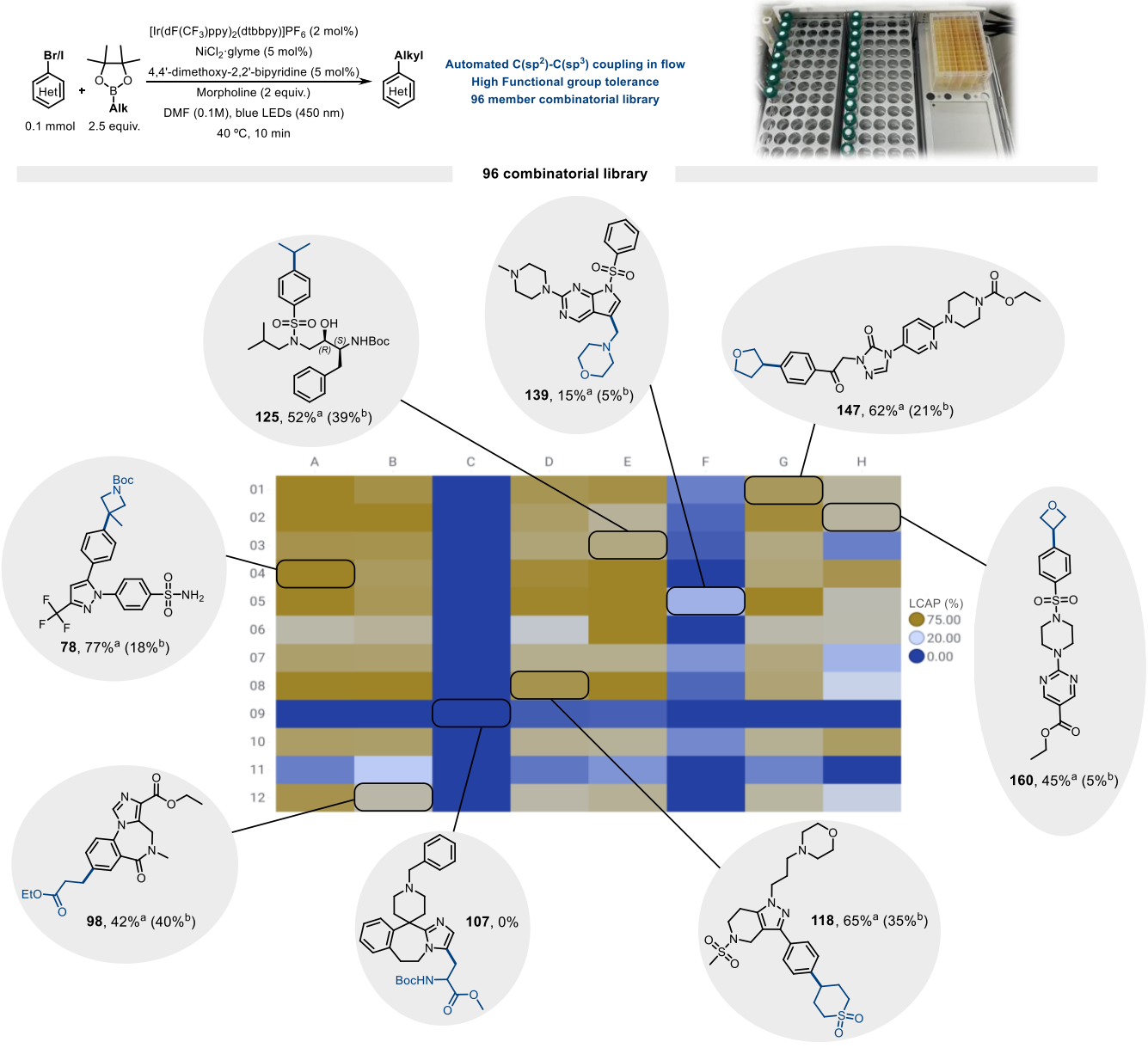

Encouragingly, we achieved a 75% success rate, enabling the preparation of 20 new products in 8 hours (equivalent to 3 products per hour). Various coupling partners bearing diverse functionalities were successfully introduced, including primary amides (**52**), lactams (**66**), nitriles (**5**, **67** and **69**), benzyl substituents (**51** and **63**), ethers (**53**, **55**, **61** and **65**), protected (**57**, **60**) and unprotected amines (**59**, **64**, **68**), allyl (**74**) and aliphatic substituents such as methyl (**71**), ethyl (**72**), cyclobutyl (**73**) or methylene cyclohexyl (**56**). However, alkyl fragments with strong electron-withdrawing groups in α-position failed (sulfonamide **54**, sulphone **62** and phosphate **70**) failed to yield significant product, with only traces observed under the optimized reaction conditions.

Having established the viability of this flow platform for library synthesis, we aimed to leverage its capabilities further by conducting a 96-member combinatorial library, linking 8 scaffolds with 12 aliphatic boronic esters. This combinatorial library incorporated a range of drug-like scaffolds, including the previously mentioned precursor of Celebrex (Scaffold **A**), an analog of flumazenil (Scaffold **B**), and 6 additional drug-like scaffolds. The 96-member combinatorial library was run in 32 hours (equivalent to 3 products per hour), achieving a remarkable diversity of coupling partners and obtaining a 55% success rate (Figure 5, SI figure S25). Notably, the flow platform gave rise to similar yields compared to the batch counterpart described herein for the same substrates (SI Table S20).

As a general observation, two aliphatic fragments consistently failed in the ART coupling, such as the amino acid derivative (e.g., **83**) and a methyl cyclopropyl fragment (e.g., **85**). All the other substituents containing diverse functionalities provided generally acceptable yields, including ethers, carbamates, morpholines, amides, sulfones, esters, and simple alkyl substituents. However, drug-like scaffold (**C**) and scaffold (**F**) posed significant challenges, as they are highly electron-rich 5-membered heteroaryl halides. Nevertheless, scaffold (**D**), containing a (sp^3)-hybridized nitrogen atom, successfully reacted with most alkyl fragments and could be isolated in moderate to good yields. Such N_{sp3} centers are known to be particularly challenging in photoredox-catalyzed couplings due to their involvement in single electron transfer (SET) events.[45]

Other highly elaborated scaffolds also yielded their desired products in, acceptable yields irrespective of their diverse functionalities (e.g., ketones, pyridines, piperazines, esters, sulfonamides, or unprotected alcohols among others). These results position this methodology as alternative to other traditional metal-catalyzed couplings such as Negishi or Suzuki couplings.[45] Importantly, despite the generally low solubility of scaffolds (**G**) and (**H**), it should be noted that there was no clogging of the flow system, and conversion towards the desired products was observed.

Conclusion

In summary, we conducted a systematic comparison of commercially available photoreactors with a focus on issues encountered with high-throughput chemistry: irradiation uniformity, reproducibility, and temperature control. Temperature emerged as a key variable in achieving desired product formation and minimizing byproducts; while all reactors provided desired product, temperature-controlled photoreactors consistently outperformed. Batch photoreactors **P6** and **P7** provided the highest conversions to desired product while minimizing byproducts, and with minimal variation across reactor positions. These characteristics fits for HTE applications including data generation campaigns to train AI/ML models, although unusual plate format (48 position) presents challenges for automated platforms. Photoreactor **P2**, despite lacking temperature control and exhibiting greater byproduct formation, achieves irradiation homogeneity and could successfully be integrated into an automated liquid handler because of its standard plate configuration and result compatible to the reaction scale of parallel medicinal chemistry. None of the commercially available photoreactors achieved temperature control at this larger scale.

In addition to assessing high throughput photochemistry batch reactors, we developed a continuous flow platform suitable for both HTE screenings and library synthesis. This platform leverages the advantages of flow chemistry, where small diameter tubing ensures uniform light irradiation and enhanced photon efficiency. Additionally, the large volume-to-surface ratio enables excellent temperature control, contributing to high reproducibility and robustness across a run of 96 experiments. However, the sequential nature of flow experiments necessitates short residence times to minimize the total experiment duration. The current platform requires relatively large injection volumes, which is an issue when starting materials are in limited supply. This may impose limitations on throughput, or the number of experiments conducted in flow. A platform combining slug flow with the ability to run at library scale would address this limitation.

The photochemical reactors in this study exhibit unique strengths and limitations, and our results help to identify the research applications where each reactor may be optimal. In addition, the data point toward future directions in reactor engineering and innovation.
For instance, a chilled 24-position parallel photoreactor would add value, occupying a reaction scale large enough for traditional medicinal chemistry, coupled with the data robustness required for AI/ML applications. Moreover, integrating these photoreactors into automated synthesis platforms (SBS-format) could enhance reproducibility by minimizing human interventions. Although technically challenging to construct, higher-density plates (>96 positions) with uniform irradiation and precise temperature control have the potential to transform data generation for AI-ML and reaction discovery.

ASSOCIATED CONTENT

Supporting Information

A detailed methods section is available in the Supporting Information and all the supplemental figures and tables referenced in the manuscript.

AUTHOR INFORMATION

Corresponding Author (*)

Santiago Cañellas − Chemical Capabilities, Analytical & Purification, Global Discovery Chemistry. Janssen-Cilag, S.A., E-45007 Toledo, Spain. https://orcid.org/0000-0002-8700-4615

Email: scanella@its.jnj.com

Authors

Brenda Pijper – Chemical Capabilities, Analytical & Purification, Global Discovery Chemistry. Janssen-Cilag, S.A., E-45007 Toledo, Spain. https://orcid.org/0000-0002-1302-7865

Lucía M. Saavedra − Chemical Capabilities, Analytical & Purification, Global Discovery Chemistry. Janssen-Cilag, S.A., E-45007 Toledo, Spain.

Matteo Lanzi − Institute of Chemical Research of Catalonia (ICIQ), the Barcelona Institute of Science and Technology, Av. Països Catalans 16, 43007 Tarragona, Spain. https://orcid.org/0000-0003-0254-7977

Maialen Alonso − Chemical Capabilities, Analytical & Purification, Global Discovery Chemistry. Janssen-Cilag, S.A., E-45007 Toledo, Spain. https://orcid.org/0000-0002-5279-2578

Alberto Fontana − Chemical Capabilities, Analytical & Purification, Global Discovery Chemistry. Janssen-Cilag, S.A., E-45007 Toledo, Spain. https://orcid.org/0000-0001-9529-9698

Marta Serrano − Chemical Capabilities, Analytical & Purification, Global Discovery Chemistry. Janssen-Cilag, S.A., E-45007 Toledo, Spain. https://orcid.org/0000-0001-9910-8879

José Enrique Gómez − Chemical Capabilities, Analytical & Purification, Global Discovery Chemistry. Janssen-Cilag, S.A., E-45007 Toledo, Spain. https://orcid.org/0000-0001-7465-0776

Arjan W. Kleij − Institute of Chemical Research of Catalonia (ICIQ), the Barcelona Institute of Science and Technology, Av. Països Catalans 16, 43007 Tarragona, Spain. Catalan Institute of Research and Advanced Studies (ICREA), Pg. Lluís Companys 23, 08010 Barcelona, Spain. https://orcid.org/0000-0002-7402-4764

Jesús Alcázar − Chemical Capabilities, Analytical & Purification, Global Discovery Chemistry. Janssen-Cilag, S.A., E-45007 Toledo, Spain. https://orcid.org/0000-0002-2726-196X

Notes

The authors declare no competing financial interest.

ACKNOWLEDGMENT

We would like to thank Raquel Rodriguez and Lucia Alcaide for providing support with the analysis and purification of the compounds, and Jose Manuel Alonso and Belén Chaves Arquero for the NMR support. An extended thanks to Peter Buijnsters, Zhicai Shi, and Scott Wolkenberg for meaningful scientific discussions. Additionally, we are grateful to the European Union for funding under the PhotoReAct Project, H2020 Marie Sklodowska-Curie grant agreement No 956324 (MSCA ITN: Pho-toReAct), the ICIQ-CERCA Program/Generalitat de Catalunya, ICREA, MICINN (PID2020-112684GB-100 and CEX2019-000925-S) and the AGAUR (2021-SGR-00853 and Beatriu de Pinós program 2021-BP-00162) for the support.

ABBREVIATIONS

API, active pharmaceutical ingredient; HTE, high-throughput experimentation; PMC, parallel medicinal chemistry; AI-ML, artificial intelligence – machine learning; ART, amino radical transfer; XEC, cross-electrophile coupling; SI, Supporting Information; DMF, dimethylformamide; Bpins, boronic esters; SBS format, Society for Biomolecular Screening dimensional standards of a microplate; LCMS, liquid chromatography-mass spectrometry; SET, single electron transfer; LED, light-emitting diode; HTP, high-throughput purification.

REFERENCES

(1) Barber, J. Photosynthetic Energy Conversion: Natural and Artificial. *Chem. Soc. Rev.* **2009**, *38* (1), 185–196. https://doi.org/10.1039/B802262N.

(2) Ghosh, I.; Marzo, L.; Das, A.; Shaikh, R.; König, B. Visible Light Mediated Photoredox Catalytic Arylation Reactions. *Acc. Chem. Res.* **2016**, *49* (8), 1566–1577. https://doi.org/10.1021/acs.accounts.6b00229.

(3) Shaw, M. H.; Twilton, J.; MacMillan, D. W. C. Photoredox Catalysis in Organic Chemistry. *J. Org. Chem.* **2016**, *81* (16), 6898–6926. https://doi.org/10.1021/acs.joc.6b01449.

(4) Prier, C. K.; Rankic, D. A.; MacMillan, D. W. C. Visible Light Photoredox Catalysis with Transition Metal Complexes: Applications in Organic Synthesis. *Chem. Rev.* **2013**, *113* (7), 5322–5363. https://doi.org/10.1021/cr300503r.

(5) Twilton, J.; Le, C.; Zhang, P.; Shaw, M. H.; Evans, R. W.; MacMillan, D. W. C. The Merger of Transition Metal and Photocatalysis. *Nat Rev Chem* **2017**, *1* (7), 0052. https://doi.org/10.1038/s41570-017-0052.

(6) Lanzi, M.; Santacroce, V.; Balestri, D.; Marchiò, L.; Bigi, F.; Maggi, R.; Malacria, M.; Maestri, G. Visible-Light-Promoted Polycyclizations of Dienynes. *Angew. Chem. Int. Ed.* **2019**, *58* (20), 6703–6707. https://doi.org/10.1002/anie.201902837.

(7) Ruffoni, A.; Juliá, F.; Svejstrup, T. D.; McMillan, A. J.; Douglas, J. J.; Leonori, D. Practical and Regioselective Amination of Arenes Using Alkyl Amines. *Nat. Chem.* **2019**, *11* (5), 426–433. https://doi.org/10.1038/s41557-019-0254-5.

(8) U. Dighe, S.; Juliá, F.; Luridiana, A.; Douglas, J. J.; Leonori, D. A Photochemical Dehydrogenative Strategy for Aniline Synthesis. *Nature* **2020**, *584* (7819), 75–81. https://doi.org/10.1038/s41586-020-2539-7.

(9) Lanzi, M.; Merad, J.; Boyarskaya, D. V.; Maestri, G.; Allain, C.; Masson, G. Visible-Light-Triggered C–C and C–N Bond Formation by C–S Bond Cleavage of Benzylic Thioethers. *Org. Lett.* **2018**, *20* (17), 5247–5250. https://doi.org/10.1021/acs.orglett.8b02196.

(10) Liu, W.; Lavagnino, M. N.; Gould, C. A.; Alcázar, J.; MacMillan, D. W. C. A Biomimetic S_H2 Cross-Coupling Mechanism for Quaternary Sp^3-Carbon Formation. *Science* **2021**, *374* (6572), 1258–1263. https://doi.org/10.1126/science.abl4322.

(11) Sandfort, F.; Strieth-Kalthoff, F.; Kühnemund, M.; Beecks, C.; Glorius, F. A Structure-Based Platform for Predicting Chemical Reactivity. *Chem* **2020**, *6* (6), 1379–1390. https://doi.org/10.1016/j.chempr.2020.02.017.

(12) Kappe, C. O. My Twenty Years in Microwave Chemistry: From Kitchen Ovens to Microwaves That Aren't Microwaves. *The Chemical Record* **2019**, *19* (1), 15–39. https://doi.org/10.1002/tcr.201800045.

(13) Alonso, M.; Cañellas, S.; Delgado, F.; Serrano, M.; Diéguez-Vázquez, A.; Gómez, J. E. Accelerated Synthesis of Bicyclo[1.1.1]Pentylamines: A High-Throughput Approach. Organic Letters 2023, 25 (5), 771-776. https://doi.org/10.1021/acs.orglett.2c04226.

(14) Le, C. C.; Wismer, M. K.; Shi, Z.-C.; Zhang, R.; Conway, D. V.; Li, G.; Vachal, P.; Davies, I. W.; MacMillan, D. W. C. A General Small-Scale Reactor To Enable Standardization and Acceleration of Photocatalytic Reactions. *ACS Cent Sci* **2017**, *3* (6), 647–653. https://doi.org/10.1021/acscentsci.7b00159.

(15) Cañellas, S.; Nuño, M.; Speckmeier, E. Improving Reproducibility of Photocatalytic Reactions—How to Facilitate Broad Application of New Methods. *Nat Commun* **2024**, *15* (1), 307. https://doi.org/10.1038/s41467-023-44362-0.

(16) Gesmundo, N. J.; Rago, A. J.; Young, J. M.; Keess, S.; Wang, Y. At the Speed of Light: The Systematic Implementation of Photoredox Cross-Coupling Reactions for Medicinal Chemistry Research. *J. Org. Chem.* **2024**. https://doi.org/10.1021/acs.joc.3c02351.

(17) Qi, N.; Wismer, M. K.; Conway, D. V.; Krska, S. W.; Dreher, S. D.; Lin, S. Development of a High Intensity Parallel Photoreactor for High Throughput Screening. *React. Chem. Eng.* **2022**, *7* (2), 354–360. https://doi.org/10.1039/D1RE00317H.

(18) Speckmeier, E.; Maier, T. C. ART─An Amino Radical Transfer Strategy for C(Sp2)–C(Sp3) Coupling Reactions, Enabled by Dual Photo/Nickel Catalysis. *J. Am. Chem. Soc.* **2022**, *144* (22), 9997–10005. https://doi.org/10.1021/jacs.2c03220.

(19) Liu, W.; Mulhearn, J.; Hao, B.; Cañellas, S.; Last, S.; Gómez, J. E.; Jones, A.; De Vera, A.; Kumar, K.; Rodríguez, R.; Van Eynde, L.; Strambeanu, I. I.; Wolkenberg, S. E. Enabling Deoxygenative C(Sp2)-C(Sp3) Cross-Coupling for Parallel Medicinal Chemistry.

ACS Med. Chem. Lett. **2023**, *14* (6), 853–859. https://doi.org/10.1021/acsmedchemlett.3c00118.

(20) A Matter of Life(Time) and Death. *ACS Catal.* **2018**, *8* (9), 8597–8599. https://doi.org/10.1021/acscatal.8b03199.

(21) Everson, D. A.; Weix, D. J. Cross-Electrophile Coupling: Principles of Reactivity and Selectivity. *J. Org. Chem.* **2014**, *79* (11), 4793–4798. https://doi.org/10.1021/jo500507s.

(22) Weix, D. J. Methods and Mechanisms for Cross-Electrophile Coupling of Csp2 Halides with Alkyl Electrophiles. *Acc. Chem. Res.* **2015**, *48* (6), 1767–1775. https://doi.org/10.1021/acs.accounts.5b00057.

(23) Sakai, H. A.; Liu, W.; Le, C. "Chip"; MacMillan, D. W. C. Cross-Electrophile Coupling of Unactivated Alkyl Chlorides. *J. Am. Chem. Soc.* **2020**, *142* (27), 11691–11697. https://doi.org/10.1021/jacs.0c04812.

(24) Zuo, Z.; Ahneman, D. T.; Chu, L.; Terrett, J. A.; Doyle, A. G.; MacMillan, D. W. C. Merging Photoredox with Nickel Catalysis: Coupling of α-Carboxyl Sp^3 -Carbons with Aryl Halides. *Science* **2014**, *345* (6195), 437–440. https://doi.org/10.1126/science.1255525.

(25) Yavorskyy, A.; Shvydkiv, O.; Hoffmann, N.; Nolan, K.; Oelgemöller, M. Parallel Microflow Photochemistry: Process Optimization, Scale-up, and Library Synthesis. *Org. Lett.* **2012**, *14* (17), 4342–4345. https://doi.org/10.1021/ol301773r.

(26) Donnelly, K.; Baumann, M. Scalability of Photochemical Reactions in Continuous Flow Mode. *J Flow Chem* **2021**, *11* (3), 223–241. https://doi.org/10.1007/s41981-021-00168-z.

(27) Harper, K. C.; Moschetta, E. G.; Bordawekar, S. V.; Wittenberger, S. J. A Laser Driven Flow Chemistry Platform for Scaling Photochemical Reactions with Visible Light. *ACS Cent. Sci.* **2019**, *5* (1), 109–115. https://doi.org/10.1021/acscentsci.8b00728.

(28) Buglioni, L.; Raymenants, F.; Slattery, A.; Zondag, S. D. A.; Noël, T. Technological Innovations in Photochemistry for Organic Synthesis: Flow Chemistry, High-Throughput Experimentation, Scale-up, and Photoelectrochemistry. *Chem. Rev.* **2022**, *122* (2), 2752–2906. https://doi.org/10.1021/acs.chemrev.1c00332.

(29) Plutschack, M. B.; Pieber, B.; Gilmore, K.; Seeberger, P. H. The Hitchhiker's Guide to Flow Chemistry. *Chem. Rev.* **2017**, *117* (18), 11796–11893. https://doi.org/10.1021/acs.chemrev.7b00183.

(30) Gioiello, A.; Piccinno, A.; Lozza, A. M.; Cerra, B. The Medicinal Chemistry in the Era of Machines and Automation: Recent Advances in Continuous Flow Technology. *J. Med. Chem.* **2020**, *63* (13), 6624–6647. https://doi.org/10.1021/acs.jmedchem.9b01956.

(31) Bogdan, A. R.; Dombrowski, A. W. Emerging Trends in Flow Chemistry and Applications to the Pharmaceutical Industry. *J. Med. Chem.* **2019**, *62* (14), 6422–6468. https://doi.org/10.1021/acs.jmedchem.8b01760.

(32) Hughes, D. L. Applications of Flow Chemistry in Drug Development: Highlights of Recent Patent Literature. *Org. Process Res. Dev.* **2018**, *22* (1), 13–20. https://doi.org/10.1021/acs.oprd.7b00363.

(33) Sun, A. C.; Steyer, D. J.; Allen, A. R.; Payne, E. M.; Kennedy, R. T.; Stephenson, C. R. J. A Droplet Microfluidic Platform for High-Throughput Photochemical Reaction Discovery. *Nat Commun* **2020**, *11* (1), 6202. https://doi.org/10.1038/s41467-020-19926-z.

(34) Sun, A. C.; Steyer, D. J.; Robinson, R. I.; Ginsburg-Moraff, C.; Plummer, S.; Gao, J.; Tucker, J. W.; Alpers, D.; Stephenson, C. R. J.; Kennedy, R. T. High-Throughput Optimization of Photochemical Reactions Using Segmented-Flow Nanoelectrospray-Ionization Mass Spectrometry. *Angewandte Chemie International Edition* **2023**, *62* (28), e202301664. https://doi.org/10.1002/anie.202301664.

(35) Chatterjee, S.; Guidi, M.; Seeberger, P. H.; Gilmore, K. Automated Radial Synthesis of Organic Molecules. *Nature* **2020**, *579* (7799), 379–384. https://doi.org/10.1038/s41586-020-2083-5.

(36) Hsieh, H.-W.; Coley, C. W.; Baumgartner, L. M.; Jensen, K. F.; Robinson, R. I. Photoredox Iridium–Nickel Dual-Catalyzed Decarboxylative Arylation Cross-Coupling: From Batch to Continuous Flow via Self-Optimizing Segmented Flow Reactor. *Org. Process Res. Dev.* **2018**, *22* (4), 542–550. https://doi.org/10.1021/acs.oprd.8b00018.

(37) Mousseau, J. J.; Perry, M. A.; Bundesmann, M. W.; Chinigo, G. M.; Choi, C.; Gallego, G.; Hicklin, R. W.; Hoy, S.; Limburg, D. C.; Sach, N. W.; Zhang, Y. Automated Nanomole-Scale Reaction Screening toward Benzoate Bioisosteres: A Photocatalyzed Approach to Highly Elaborated Bicyclo[1.1.1]Pentanes. *ACS Catal.* **2022**, *12* (1), 600–606. https://doi.org/10.1021/acscatal.1c05076

(38) Slattery, A.; Wen, Z.; Tenblad, P.; Sanjosé-Orduna, J.; Pintossi, D.; den Hartog, T.; Noël, T. Automated Self-Optimization, Intensification, and Scale-up of Photocatalysis in Flow. *Science* **2024**, *383* (6681), eadj1817. https://doi.org/10.1126/science.adj1817.

(39) Pijper, B.; Abdiaj, I.; Leonori, D.; Alcázar, J. Development of an Automated Platform for C(Sp3)−C(Sp3) Bond Formation via XAT Chemistry. *ChemCatChem* **2023**, *15* (4), e202201289. https://doi.org/10.1002/cctc.202201289.

(40) Abdiaj, I.; Cañellas, S.; Dieguez, A.; Linares, M. L.; Pijper, B.; Fontana, A.; Rodriguez, R.; Trabanco, A.; Palao, E.; Alcázar, J. End-to-End Automated Synthesis of C(Sp3)-Enriched Drug-like Molecules via Negishi Coupling and Novel, Automated Liquid–Liquid Extraction. *J. Med. Chem.* **2023**, *66* (1), 716–732. https://doi.org/10.1021/acs.jmedchem.2c01646.

(41) Hashem, M. M.; Berlin, K. D.; Chesnut, R. W.; Durham, N. N. Novel Pyrazolo, Isoxazolo, and Thiazolo Steroidal Systems and Model Analogs Containing Dimethoxylaryl (or Dihydroxylaryl) Groups and Derivatives. Synthesis, Spectral Properties, and Biological Activity. *J. Med. Chem.* **1976**, *19* (2), 229–239. https://doi.org/10.1021/jm00224a007.

(42) Scott, S. L.; Gunnoe, T. B.; Fornasiero, P.; Crudden, C. M. To Err Is Human; To Reproduce Takes Time. *ACS Catal.* **2022**, *12* (6), 3644–3650. https://doi.org/10.1021/acscatal.2c00967.

(43) Degorce, S. L.; Bodnarchuk, M. S.; Scott, J. S. Lowering Lipophilicity by Adding Carbon: AzaSpiroHeptanes, a logD Lowering Twist. *ACS Med. Chem. Lett.* **2019**, *10* (8), 1198–1204. https://doi.org/10.1021/acsmedchemlett.9b00248.

(44) Cauley, A. N.; Ramirez, A.; Barhate, C. L.; Donnell, A. F.; Khandelwal, P.; Sezen-Edmonds, M.; Sherwood, T. C.; Sloane, J. L.; Cavallaro, C. L.; Simmons, E. M. Ni/Photoredox-Catalyzed C(Sp2)–C(Sp3) Cross-Coupling of Alkyl Pinacolboronates and (Hetero)Aryl Bromides. *Org. Lett.* **2022**, *24* (31), 5663–5668. https://doi.org/10.1021/acs.orglett.2c01942.

(45) Dombrowski, A. W.; Gesmundo, N. J.; Aguirre, A. L.; Sarris, K. A.; Young, J. M.; Bogdan, A. R.; Martin, M. C.; Gedeon, S.; Wang, Y. Expanding the Medicinal Chemist Toolbox: Comparing Seven C(Sp2)–C(Sp3) Cross-Coupling Methods by Library Synthesis. *ACS Med. Chem. Lett.* **2020**, *11* (4), 597–604. https://doi.org/10.1021/acsmedchemlett.0c00093.

For Table of contents only